The Boulder Atmospheric Observatory

J. C. KAIMAL AND J. E. GAYNOR

NOAA/ERL/Wave Propagation Laboratory, Boulder, CO 80303

(Manuscript received 16 September 1982)

ABSTRACT

The Boulder Atmospheric Observatory (BAO) is a unique research facility for studying the planetary boundary layer and for testing and calibrating atmospheric sensors. The facility includes a 300 m tower instrumented with fast- and slow-response sensors, a variety of remote sensing systems, and a real-time processing and display capability that greatly reduces analysis time for scientists working with current or archived data. In the past four years of operation the BAO has been the site of several large cooperative experiments and numerous smaller ones. Details of the data acquisition, processing and archiving schemes are presented. Results of studies conducted and opportunities for future investigations are also described.

1. Introduction

Located on gently rolling terrain 25 km east of the foothills of the Colorado Rockies, the Boulder Atmospheric Observatory (BAO) is a research facility operated by NOAA for studying the planetary boundary layer and for testing and calibrating atmospheric sensors. The BAO is situated on a section of agricultural land halfway between the Boulder valley on the west and the South Platte river basin on the east (see topographical map in Fig. 1). It is within easy commuting distance from the urban centers of Boulder, Denver and Longmont. The terrain in the immediate area is reasonably flat with gentle slopes to the north, east and west. The steepest gradient (7%) is to the south, in the direction of a small hill.

Originally conceived as a joint meteorological observing facility for scientists at NOAA's Wave Propagation Laboratory (WPL) and the National Center for Atmospheric Research (NCAR), the facility continues to serve as a base for coordinated observational programs by government agencies, universities, private organizations and international groups. In our four years of operation, the 300 m instrumented tower and its data acquisition system have been augmented by the addition of a broad range of remote sensors, opening the way for long-range programs in plume diffusion, cloud precipitation and boundary layer parameterization studies.

2. Facilities at the BAO

The 300 m tower at the site is a guyed open lattice structure of uniform triangular cross section with legs spaced 3 m apart. A three-person elevator inside the tower provides access to the eight instrumentation levels while a movable carriage on the WSW face offers the option of continuous profiling or fixed-level operation at any desired height. Details of the tower design are given by Hall (1977). A small modular building and a complex of trailers at the base of the tower house the office and work areas for BAO staff and visitors, our on-site calibration facility, and our data acquisition system. Six-hundred meters SSW of the tower (Fig. 2), a fenced-in 50 m^2 area is provided for semipermanent installation of some of WPL's remote sensor systems. It also serves as a temporary parking area for instrument trailers brought in for special experiments.

The 300 m height of the tower ensures that instruments extend above the nocturnal planetary boundary layer nearly all of the time and to at least 25% of the daytime convective boundary layer around mid-afternoon on most of the days. There are occasions when, in the presence of strong subsidence, the daytime capping inversion stays within the tower height; these are invariably associated with strong air pollution episodes in the Denver area. On most days, however, the capping inversion is observed within the tower height until late morning, after which it rises abruptly to a height somewhere typically between 1000 and 1500 m.

The instrumentation levels on the tower are distributed linearly with height except for the two lowest levels. The booms are set at 10, 22, 50, 100, 150, 200, 250 and 300 m. Two booms are provided at each level (see Fig. 3) for easy switching of the turbulence sensors from the SSE to the NNW booms so as to take advantage of the shift in prevailing wind direction at the site between summer and winter. Fine adjustments on the boom permit leveling of sensors on it to within 0.1° of horizontal. For servicing, the horizontal brace is detached and the boom swung toward one face of the tower and retracted, to bring

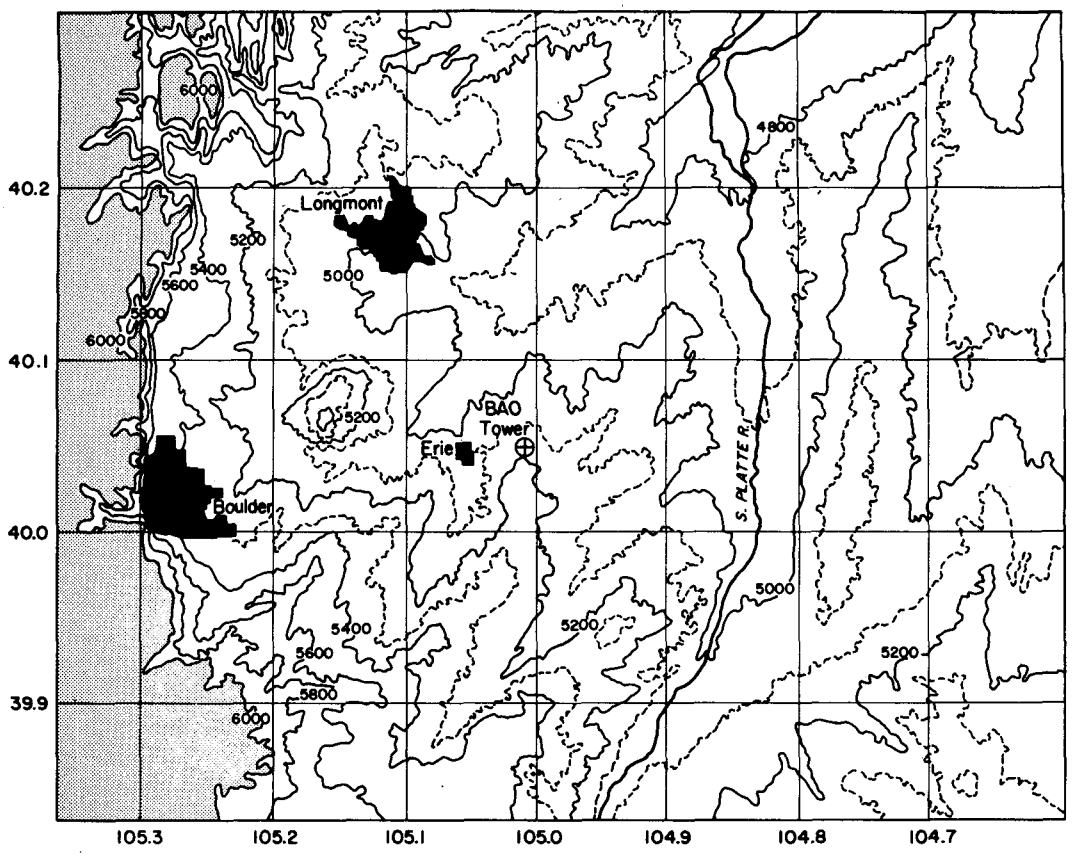

FIG. 1. Contour map of the area around the Boulder Atmospheric Observatory. Contours are indicated in feet; the stippled area represent elevations above 6000 ft. Markings around the frame are the latitudes (N) and longitudes (W).

the sensors within easy reach from the platform at each level.

Standard measurements on the tower are listed in Table 1. At each level a three-axis sonic anemometer measures wind velocity components along three orthogonal directions. The configuration of the acoustic array (see Fig. 4a) permits a wider, unobstructed azimuth coverage for both the vertical component axis and the platinum wire thermometer nestled in it than in the nonorthogonal configuration (Kaimal *et al.*, 1974; Mitsuta, 1974) used in past surface layer experiments.

This new array has its own limitations. The spatial separation between the vertical and the horizontal paths inevitably degrades the high-frequency response (wavelength $\lambda < 3$ m) in stress measurements, not a serious limitation for measurements at 10 m and above. In the atmosphere's surface layer, the stress contribution at $\lambda < z/3$ is usually negligible (Kaimal *et al.*, 1972) except in extremely stable stratification. The other limitation is the shadowing of the acoustic path by transducers in the horizontal array; the measured velocities are systematically underestimated as the wind direction approaches either of the array axes. A simple algorithm in the data acquisition software corrects this error in real time. The effect of the transducer blockage on the measurement and the correction algorithm used are given in Appendix A.

The sonic anemometers at all levels are pulsed synchronously 200 times per second. While each pulse provides a separate wind velocity reading, only 20-point nonoverlapping block averages of the readings are presented (every 0.1 s) to the output registers for transfer to the data acquisition system. This built-in block averaging is designed to minimize aliasing in spectra computed from the time series; in addition, it improves the effective velocity resolution[1] in the measurements.

The fast-response temperature sensor[2] used in conjunction with the sonic anemometer consists of a simple bridge circuit with a length of 12 μm platinum wire ($\sim$150 Ω resistance at 20°C) on one of its legs. The wire is wound on a helical bobbin attached to the end of a 10 cm rod (see Fig. 4a). The mechanical

[1] The velocity resolution with our 10 MHz timing clock is 0.03 m s^{-1} per reading and 0.007 m s^{-1} for the averaged data point.

[2] Atmospheric Instrumentation Research, Inc., Model DT1A.

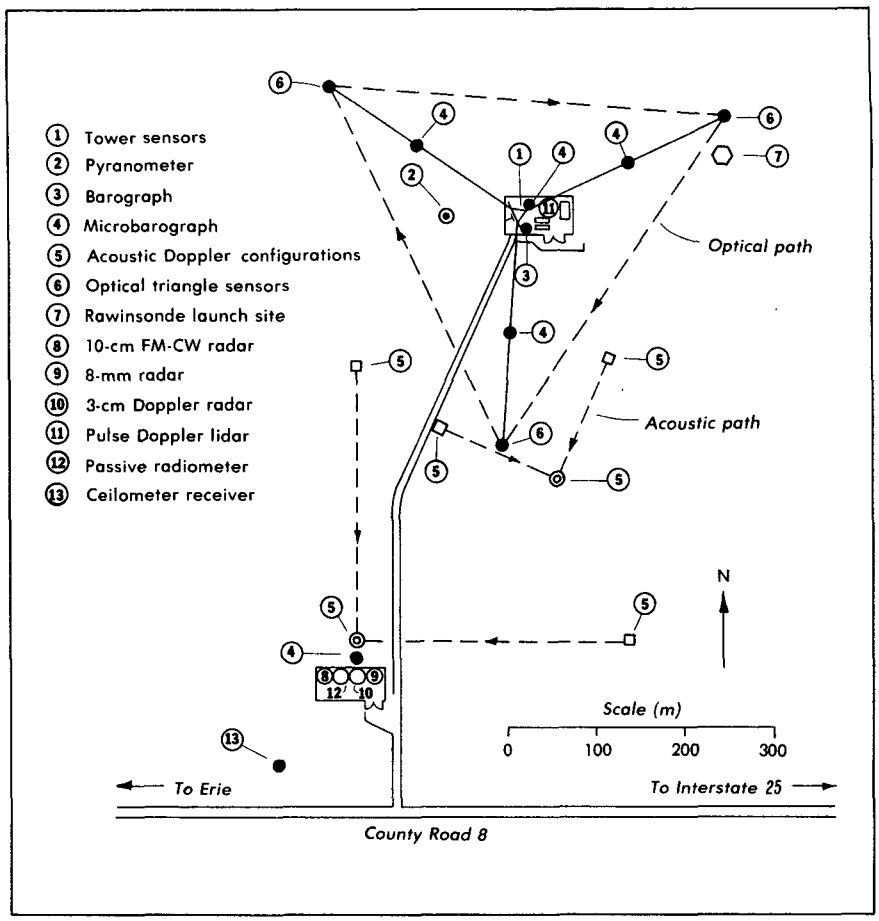

FIG. 2. Plot plan of the BAO site showing location of the various sensors and facilities.

support provided by the bobbin adds considerably to the useful life of the wire without degrading its frequency response in the 0–5 Hz range needed for turbulent flux measurements. Unless hit by debris or exposed to freezing rain the wire will operate intact for weeks at a time. The low-noise, low-drift electronic circuitry in the temperature sensor has an output range of ±10 V corresponding to a temperature range of ±50°C. This wide operating range makes range switching unnecessary, but does require a high bit resolution in the analog-to-digital converter (14 binary bits in the BAO system) to maintain accuracy. A simple calibration scheme in the circuit permits readjustment of system gain and zero offset to accomodate probe-to-probe variations and the effects of aging on the platinum wire response.

The slow-response temperature sensor mounted on the SSE boom (see Fig. 4a) is a quartz thermometer[3] housed in an aspirated radiation shield.[4] By using a single reference oscillator in the detector circuit for probes at all levels, a high relative accuracy of 0.001°C between the temperature measurements is maintained. With residual radiation errors and the effect of fluctuations in the aspiration rate from windspeed changes included, the absolute accuracy in any measurement is good to within ±0.05°C.

The NNW boom supports a propeller-vane[5] anemometer and a cooled-mirror dewpoint hygrometer[6] as shown in Fig. 4b. Both sensors are calibrated periodically according to procedures outlined by the manufacturer. The propeller-vane anemometer is needed for reliable mean wind information when the wind direction is unfavorable for the sonic anemometer, i.e., blowing close to or through the tower. The polystyrene propeller used in this model has a distance constant of 2.4 m and working range from 1 to 54 m s^{-1}. The vane position is indicated by a precision, conducting-plastic potentiometer connected to the vane shaft. In positioning the potentiometer, the deadband of the potentiometer is pointed in the

[3] Hewlett-Packard, Model 2850A.
[4] R. M. Young Co., Aspirator Model 43404.
[5] R. M. Young Co., Propvane Model 8002.
[6] Cambridge Systems, Model 110 SM.

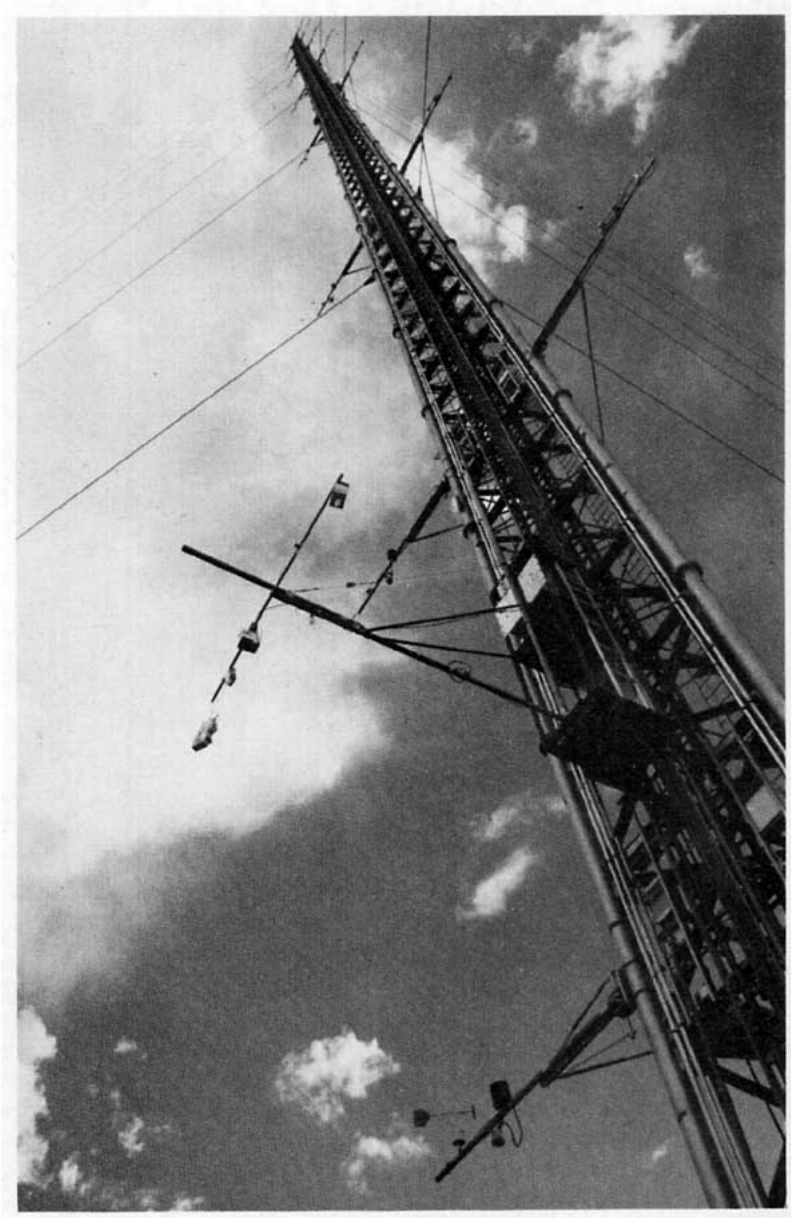

FIG. 3. View of the BAO 300 m tower showing boom configuration at the eight fixed levels and on the movable carriage. In this photograph, the carriage is being used for comparing vertical profiles of temperature and humidity measured by four radiosonde systems (see text).

direction of the tower to provide optimum coverage of winds from directions favorable to sensors on the NNW boom.

Instrumentation on the movable carriage varies with the specific requirements of each experiment. The boom attached to the carriage has, at various times, been instrumented with gas and particle samplers; free and tethered balloon packages; and sensors for tracking wind, temperature and humidity profiles across the tower height. Fig. 3 shows an array of free-balloon packages being compared on the carriage boom during a WMO-sponsored intercomparison of low-level sounding systems conducted at the BAO (Baynton *et al.*, 1981) in August 1979. Height indication is available in the form of a voltage output from a geared 10-turn potentiometer and idler wheel arrangement tracking the vertical movement of the carriage. More recently, a special scaffold was attached to the carriage (see Fig. 5) for precise gradient measurements of wind, temperature and dewpoint across a 10 m vertical distance at selected heights within the nocturnal boundary layer.

TABLE 1. BAO sensor characteristics and sampling rates.

Standard sensors	Location	Parameters measured	Rate sampled (s^{-1})	Response characteristic	Basic accuracy
Sonic anemometer	Eight levels on tower, on either boom and on carriage (as needed)	V_H, A_Z, u, v, w	10	20-point low-pass filter (~5 Hz cut-off)	>1% or >1 cm s^{-1}
Propeller-vane anemometer	All levels on opposite side from sonic anemometer and on carriage (as needed)	S, D	1	1 m distance constant	~3%
Platinum wire thermometer	All levels and on carriage (as needed) Attached to sonic probe	θ	10	5–10 Hz cut-off	~1%
Quartz thermometer	All levels on SSE boom and on carriage (as needed)	T	1	~1 min time constant	0.05°C
Cooled-mirror hygrometer	All levels on NNW boom	T_d	1	~1 s cycle time	0.5°C
Lyman-α hygrometer	On carriage and selected levels	q	10	1–2 cm path averaged	5%
Absolute pressure	Surface, near tower base	P	1	3 min time constant	1 mb
Fluctuating pressure	Five surface locations	p	1	3 min time constant	1 mb
Solar radiation	Surface, 100 m W of tower	R	1	~5 min	~5%
Optical triangle sensors	Surface, outer anchor points	S, D, convergence, C_N^2	1	Spatial average over 450 m equilateral triangle	~5%

In addition to the fixed level and carriage instrumentation described above, we have several sensors on the ground (see Fig. 2) that are also considered part of our standard sensor inventory:

1) An Eppley pyranometer mounted on a 2 m mast to detect the incoming solar radiation.

2) An absolute pressure sensor (in-house design) located in the fenced-in area at the base of the tower.

3) Five sensitive microbarographs (in-house design) for detecting pressure fluctuations associated with gravity waves located at the three inner-guy anchor points and in the two fenced-in areas.

4) An optical triangle connecting each of the three outer-guy anchor points to measure the mean surface (4 m) windspeed and direction and the convergence within the triangle. Each leg of the triangle is an optical cross-wind sensor with a transmitter and receiver at each end. The mean cross-wind velocity and the scintillation intensity (related to the temperature structure parameter C_T^2) observed along each leg are sampled at the rate of once per second in the BAO data acquisition system.

Operating off-line at the site are a tipping-bucket rain gage, a ceilometer and a rawinsonde launch facility.

In Table 2 we have a summary of the remote sensors at the site, their locations and characteristics. Of the six systems listed, only the acoustic Doppler sounder is considered a permanent component of the BAO. Facsimile recordings of the thermal structure are made routinely for archiving. The Doppler part of the system, with its microprocessor-generated listings and windspeed and direction plots is activated only when such data are needed in an experiment. The photograph in Fig. 6 shows some of the other remote sensors operating at the BAO during an upslope cloud observation experiment conducted in the spring of 1982. A description of the available remote sensors follows.

The FM-CW 10 cm radar, operating in the "range only" mode with its antenna pointing upright, is useful for monitoring the depth of the daytime boundary layer, an important parameter in atmospheric turbulence and diffusion studies. The radar detects clear air returns from the atmosphere, principally from

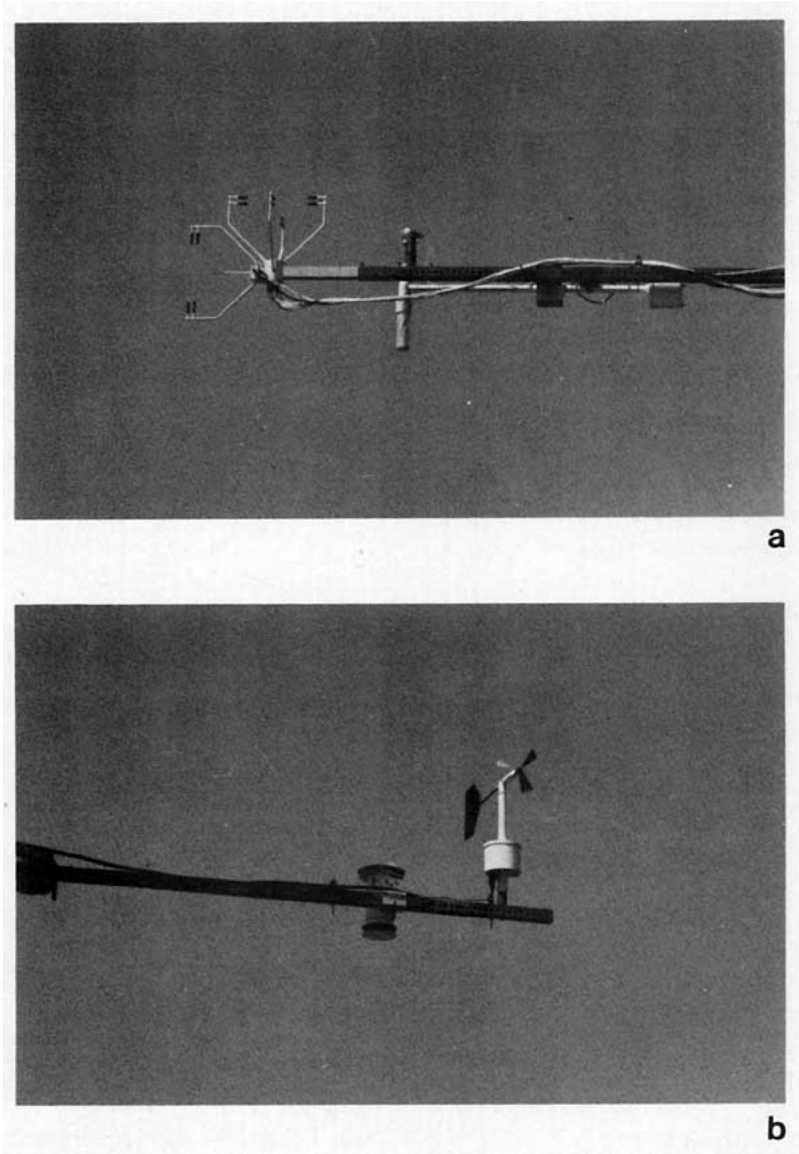

FIG. 4a. View of the three-axis sonic anemometer, the fast-response platinum wire temperature probe, and the aspirated slow-response quartz thermometer in a radiation shield, on the SSE boom.

FIG. 4b. View of the propeller vane anemometer and the cooled-mirror dewpoint hygrometer on the NNW boom.

humidity gradients and to a lesser extent from temperature gradients. Introduction of chaff or insects into the air produces strong echoes which can interfere with mixing depth estimation. In the "Doppler" mode, the radar measures radial winds: vertical (w) component with the antenna upright, and horizontal components (assuming w averages out to be zero) with a tilted antenna.

The TPQ-11 8 mm radar, modified to detect small particles in addition to cloud droplets, is also capable of measuring mixed-layer heights. However, its main application is in cloud and precipitation studies conducted at the site.

Also available for deployment at distances of 10 km from the tower are two X-band 3 cm radars which, when operated in the dual-Doppler mode, provide information on the three-dimensional wind field within a sampling volume roughly 7 km on the side and 1–2 km deep. In studies of thunderstorm dynamics and frontal development, hydrometeors serve as targets for the radars which scan in tilted planes that pass through the base line connecting the two radar stations. For boundary layer studies at the site, artificial chaff (aluminized mylar filament 1.6 cm long) is released from aircraft. The same radar is now being used in plume diffusion studies (Moninger and

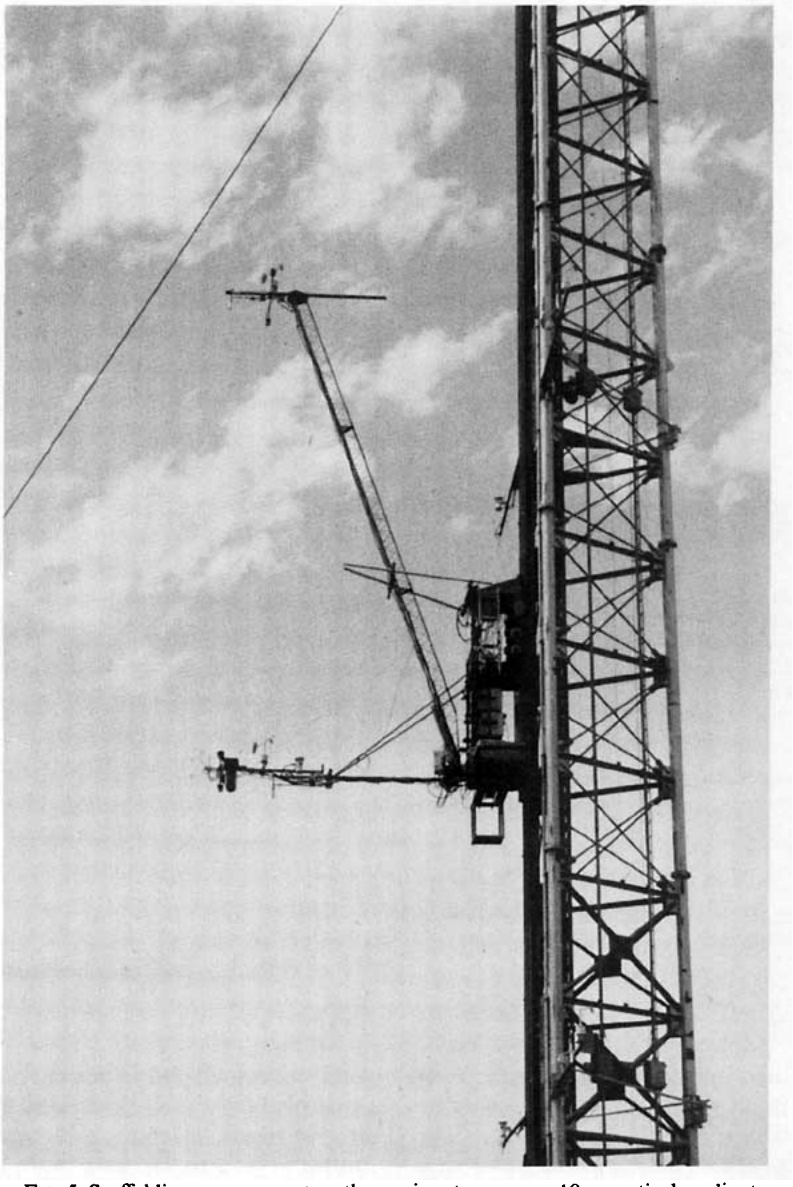

FIG. 5. Scaffolding arrangement on the carriage to measure 10 m vertical gradients of windspeed, wind direction, temperature and humidity in elevated stable layers. During BUCOE (Boulder Upslope Cloud Observation Experiment) held in the spring of 1982 (see text), particle counters were added to the array of meteorological sensors on the lower boom.

Kropfli, 1982) to track chaff released from the tower. A single radar was operated in the velocity-azimuth display mode to measure horizontal winds at the BAO site during the recent upslope cloud observation experiment (see Fig. 2).

The two-channel lidar system with dual-polarization capability is operated from a point 3 km NNW of the tower (not shown in Fig. 2) to track oil fog plumes released from the tower during diffusion experiments conducted at the BAO. The lidar operating at a 10 Hz sampling rate completes a plume scan (in range and elevation) in about 15 s. The infrared pulse-Doppler lidar (see Fig. 2), capable of measuring radial winds to distances of 10 km, is located in the fenced-in area at the base of the tower. The system is being tested for future applications in airborne and satellite remote sensing of atmospheric winds.

Installed permanently in the fenced-in area at the base of the tower are two trailers and a small modular building housing various components of the BAO (see Fig. 2). One of the trailers contains the sensor interface electronics and a data acquisition system designed around a PDP 11/34 computer. Computer peripherals include a line printer, disk drive, two

TABLE 2. WPL remote sensors at the BAO site.

Sensor type	Location	Parameters measured	Spatial resolution	Recording mode	Applications at BAO
Acoustic sounder (monostatic and Doppler bistatic)	~300 m south of tower	Temperature structure; windspeed and direction to 500 m height	20 m vertical resolution	Time-height facsimile display of temperature structure; computer processed wind speed and direction on magnetic tape	Monitoring morning inversion rise, nighttime stratifications gravity waves and boundary layer erosion events; wind sensing above tower level
FM-CW 10-cm radar (range and Doppler modes)	~600 m SSW of tower	Humidity (and to less extent temperature) inhomogeneities; radial wind velocities to 2 km	1 m for echo returns; 100 m for wind velocities	Facsimile recording on same scale as acoustic sounder and computer processed winds on tape	Monitoring daytime boundary layer depths and nighttime stratifications
TPQ-11 8 mm radar	~600 m SSW of tower	Echo intensity from particulates	75 m vertical resolution	Facsimile recording	Monitoring cloud base height, depth of daytime mixing layer
X-band radar	~600 m SSW of tower, or ~10 km from tower in direction dictated by application	Artificial chaff concentration with single radar; 3-dimensional wind field with dual-Doppler system	Volume at 10 km distance: 75 m × 200 m (diameter)	On magnetic tape for post processing	Chaff plume diffusion experiments with single radar; 3-dimensional wind field measurements for boundary layer studies
Multi-wavelength lidar (ruby and Nd:Yag with frequency doubling)	3 km NNW of tower	Backscatter echo intensity related to particle concentration	5 m radial direction	Real time display on scope, digitized readings on magnetic tape	Particle and oil fog dispersion studies; cloud studies (utilizing dual-polarization capability)
IR Doppler lidar	near base of the tower	Radial wind velocity and backscatter coefficient	300 m radial direction, beamwidth 30 μrad	On magnetic tape	Horizontal wind profiles to tropopause operating in the VAD mode

magnetic tape units, and interface for telephone linkage to a larger data processing and archiving facility in the NOAA laboratory building in Boulder. The other trailer is a calibration facility which includes a small (1 m diameter × 20 m length) wind tunnel, a constant temperature bath and a humidity chamber. All calibrations are traceable to the National Bureau of Standards. The facility is used primarily for routine verification of BAO sensor calibrations. They are also available to visiting scientists for checking the calibration of their sensors. The modular building in the northeast corner of the fenced-in area (Fig. 2) serves as a work area for the BAO technical staff stationed at the site. It also accommodates the electronic hardware for the acoustic sounder and the microbarographs.

The BAO data processing, archiving and user facility at NOAA's Environmental Research Laboratory building in Boulder receives data transmitted through phone lines from the BAO site. Here, the data are made available to users in a variety of forms. The system is designed around a PDP 11/70 computer system which includes two magnetic tape units, a line printer, a disk drive, and eight user terminals, three of which have graphics capability. Access to the computer and to the data stored in memory is possible through the user terminals mentioned above and through a limited number of phone line ports connected to the local telephone exchange.

3. Data acquisition and display

The number and types of sensors sampled at the BAO, the real-time computations performed to produce periodic data summaries, the options for on-site tape recording and the phone line transmissions to Boulder, have all contributed to produce data acquisition software of great complexity. Only a broad outline of the operations is given here. The sequence of operations is summarized in Fig. 7.

The data acquisition program samples up to 64 analog and 45 digital sensor channels. Conventional analog and digital multiplexing techniques are used to address those channels. Of the 64 analog channels

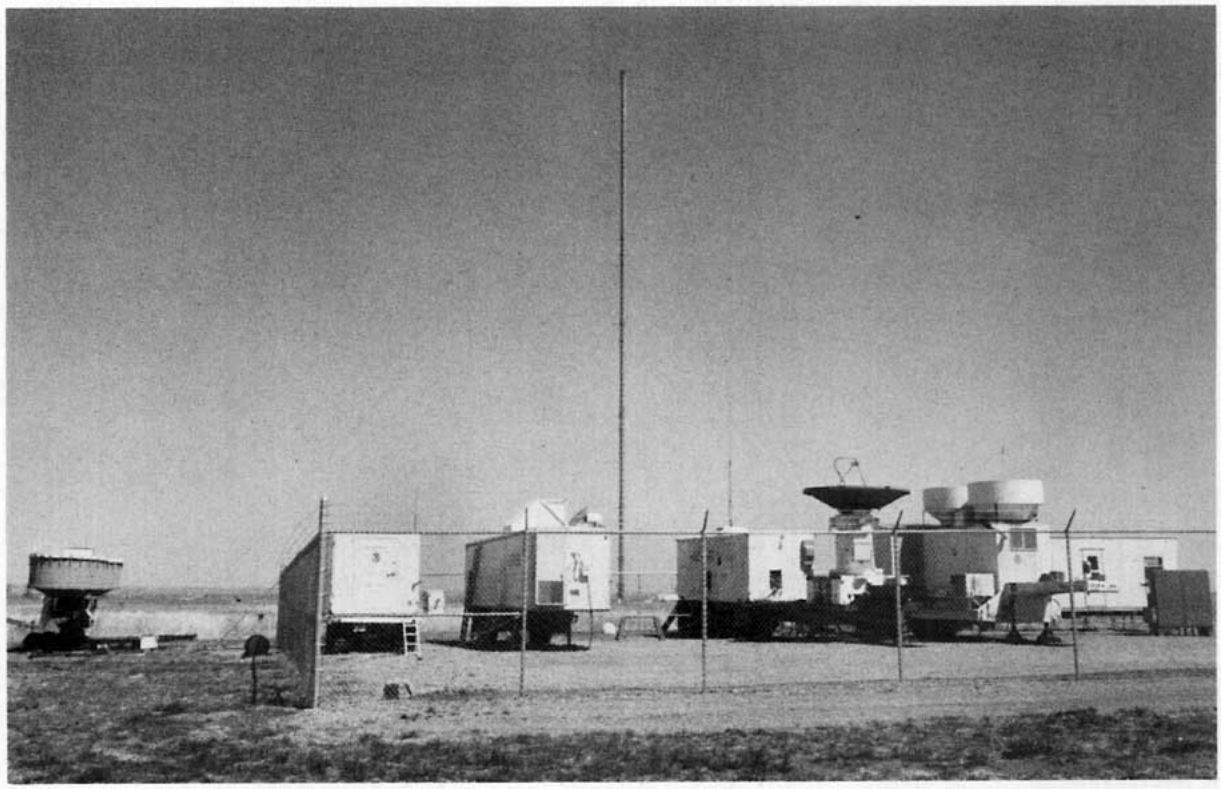

FIG. 6. Remote sensors stationed at the remote parking area 600 m SSW of the tower during BUCOE. From left to right are the FM-CW radar antenna (outside the fence), and the FM-CW radar van, the passive radiometer, the 3 cm Doppler radar, and the 8 mm radar (inside the fence).

as many as 32 can be set aside for bringing in data from special sensors that are not part of the standard instrumentation described in Section 2. These may include the carriage sensors and any other in-house or visitor device used at the site. The special channels are handled separately in the data acquisition program, and only the most basic computations for real-time listing of means and standard deviations are provided.

From the data acquisition standpoint the sensors can be divided into one of two categories: the fast-response sensors (sonic anemometers, platinum thermometers and Lyman-α hygrometers), sampled 10 times a second; and slow-response sensors (remaining sensors) sampled once per second. The software is designed to handle up to 16 fast-response and 16 slow-response special channels. In the schematic diagram of Fig. 7 only the operations performed on the standard measurements are indicated.

It was recognized from the outset that the recording and transmission of all sampled data to Boulder would place an unacceptable burden on the BAO computer systems. The problem of retaining all relevant information in the bandwidth of our measurements was solved by storing the high-frequency information (0.01–5 Hz) in the form of smoothed spectral and cospectral estimates updated every 20 min, and the low-frequency information (0–0.05 Hz) in the form of 10 s averaged time series. The spectral data saved are the averages of 10 successive 1024-point (~2 min) FFT spectral estimates, block averaged over nonoverlapping frequency intervals to produce from 7 to 10 logarithmically spaced estimates per decade. As seen in Appendix B, this procedure reduces the number of estimates needed per channel per 20 min period to 22. Spectral estimates are available for vertical velocity (w) and temperature (T); both these variables can be treated as scalar quantities. Performing the required coordinate transformation for calculating the longitudinal and lateral velocity spectra in real time is beyond the capability of our present hardware/software configuration. The high-frequency spectral information on w and T yields such parameters as the dissipation rate of turbulent kinetic energy (ϵ) and the temperature structure function (C_T^2). The data set comprising the spectral estimates of w and T and the cospectral estimates of wT are referred to in BAO parlance as the "S Data" (see Fig. 7).

The low-frequency information is retained in two parallel time series: 1) as block-averaged 10 s data points from both the slow- and the fast-response

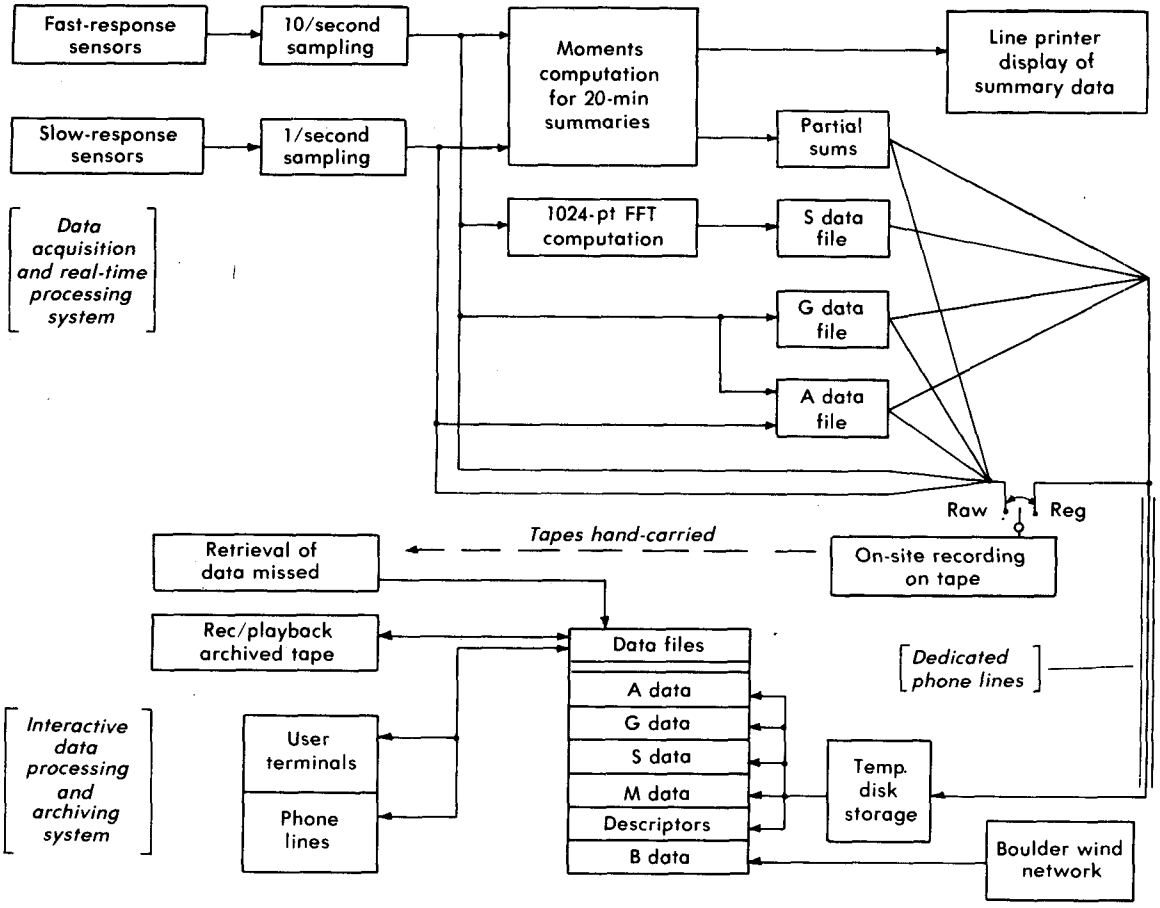

FIG. 7. Schematic diagram of the sequence of operations associated with data acquisition, data processing and archiving. See text for details.

channels and 2) as grab samples (last sample in each 10 s block) of only the fast-response channels. The averaged time series, called "A Data" in Fig. 7, is useful for a number of applications. A 512-point FFT applied to this time series provides the spectral information needed to fill in the low-frequency portion of bandwidth not covered by the S Data. Block-averaging reduces spectral distortions at the high-frequency end from aliasing, and ensures a good match between S Data spectra and A Data spectra in their region of overlap. The A Data are also useful for generating eight-level plots of fluctuations in any variable measured on the tower. This capability has proved to be invaluable both as a diagnostic tool for testing sensor failure and as an analytic tool in boundary layer studies.

The grab sample ("G Data") is saved since it contains the high-frequency turbulence information needed to obtain dependable higher order moments (e.g., variances, fluxes and third moments), not possible with the A Data. Haugen (1978) has shown that even with such widely spaced data points, it is possible to approach values within 5% of the true variances and 10% of the true fluxes if at least 60 grab samples are available for computation.

Important as our spectral analysis and time-series plots are in boundary layer studies, the most widely used BAO product is the real-time printout of data summaries updated every 20 min. The 20 min averaging periods for the summary listings start on the hour (recorded always on Mountain Standard Time). Means, variances and Obukhov lengths for all eight levels, solar radiation, pressure and summaries of the microbarograph and optical triangle measurements are computed and listed on a single sheet; the special channel means, variances and calibration constants appear on a separate sheet.

The partial sums generated in the computations for the summary listings are stored in memory along with the S, A and G Data. It is this sequence of data that we record on magnetic tape and also transmit by phone lines to the PDP 11/70 computer in Boulder. The data are recorded (and transmitted) in integer form, rather than in meteorological units, to conserve word size. As shown in Fig. 7, the data acquisition program offers a second recording option

which is used only for experiments where the need for the full time series is apparent. This option, designated RAW (for raw data) as opposed to REG (for regular data), records on tape the basic time series needed for calculating spectra of all three velocity components (u, v, w) and temperature. In this recording mode no time is available for calculating the S Data. Thus all spectral calculations have to wait until the tapes can be transported to Boulder and played back on the PDP 11/70 computer system. Special programs currently exist for extracting spectra from the RAW data tapes as well as for extracting simply the S Data to fill gaps left in the data stream received directly from the on-site data acquisition system.

Data handling in the PDP 11/70 computer system is controlled by a multi-user operating system (RSX11-M) which permits time sharing between the sorting, processing and storage operations that have to be performed on incoming data and the data analysis and program development needs of users accessing the computer through its various terminals and phone lines. Data received from the on-site data acquisition computer, understandably, receive first priority. These data are first stored in temporary locations in disk memory; at the end of every 20 min period, they are reprocessed to generate from the partial sums, summary data ("M Data") which are stored in appropriate data files along with the S, A and G Data[7]; all numbers are converted to meteorological units for user convenience and for subsequent archiving on tape. Our present disk storage capacity permits storage of only the past 1 week of data on file. The files are therefore continually updated as the older data are transferred to magnetic tapes for archiving. Retained permanently in disk memory are "descriptors" which consist of the significant 20 min averages from the M Data set, considered crucial in data searches for interesting meteorological events. (Our descriptor file dates back to the first experiments in 1978.) The descriptors include defect codes (0–9) indicating known or suspected defects in the data channels.

4. Standard user programs

A number of standard computer programs are available for inspecting and analyzing the BAO data. For the user who must perform some manipulations of the data, but does not wish to write specialized computer programs, the PIDGIN language is available. It consists of English words used singly and without syntax. The program guides the user through a series of interactive statements to provide previews of the data and perform basic manipulations and analyses on a timely basis. The convenience it offers many users often outweighs the price one pays with "overhead" in memory and processing time.

Most of the data manipulation and plotting programs are written in FORTRAN to keep the computing time within reasonable limits. A fully documented library of nearly 200 subroutines is available to the user. The user may utilize existing programs or run special programs created from subroutines residing in computer memory. Following is a summary of the major user programs tailored specifically for the BAO data sets in their various forms.

1) DATA AVAILABILITY LISTING

For most users of BAO data, the first operation would be a search in the archiving file to ascertain if data exist for the period of interest. A call for the "available data" subroutine followed by entries of data type and the starting and ending dates produces a printout of the numbers of 20 min periods of data available in each hour (0 to 3) for the days requested. Fig. 8 is a sample printout showing M Data available between 18 and 27 April 1982.

2) TWENTY-MINUTE SUMMARY LISTING

The next step would be a request for the M Data (the standard 20 min summary data) for the period of interest in order to further narrow down the event to be analyzed. The program prints out the summary listings (see Fig. 9) using data from the disk files, or from archived tapes if data requested are older than a week. The printout includes mean winds, temperatures, dewpoints and Obukhov lengths (top set), variances and turbulent fluxes (middle set) and surface pressure, radiation and optical triangle data (bottom set). Mean horizontal sonic anemometer winds are shown both as components (positive from south and west) and as vector magnitude and direction. W is the vertical wind component. The symbols U and V in the middle set are the orthogonal wind components aligned to the 10 m longitudinal and lateral wind components respectively. (The option to align the coordinate systems at each level to the flow at that height, is also available.) All numbers are in SI units unless otherwise indicated. The date-time indicated at top left denotes the beginning of the 20 min period. Not shown in the figure is a companion sheet that lists means, variances and calibration constants for the special channels.

3) TIME SERIES PLOTS

This program plots on request one to eight levels of any variable for which data exist in disk files in archived form. Fig. 10 is a sample of the vertical velocity plot for 1 h (360 A Data points starting at 0620 MST 27 March 1981). The traces follow the height

[7] Another data set called the B Data are also retained. These are derived from a network of conventional wind sensors distributed in the Boulder area for gust studies (Bedard, 1982).

AVAILABLE DATA SINCE 820611. , OF KIND M 22-JUN-82 07:49

DATE	HOUR 0	1	2	3	4	5	6	7	8	9	10	11	12	13	14	15	16	17	18	19	20	21	22	23
820611.	111	111	111	111	111	111	111	011	111	111	111	111	111	111	111	111	111	111	111	111	111	111	111	111
820612.	111	111	111	111	111	111	111	111	111	111	111	111	111	111	111	111	111	111	111	111	111	111	111	111
820613.	111	111	111	111	111	111	111	111	111	111	111	111	111	111	111	111	111	111	111	111	111	111	111	111
820614.	111	111	111	111	111	111	111	111	111	110	000	011	000	010	111	111	111	111	111	111	111	111	111	111
820615.	111	111	111	111	111	111	111	111	111	111	111	111	011	111	111	111	111	111	111	111	111	111	111	111
820616.	111	111	111	111	111	011	111	111	101	111	111	111	111	111	111	111	111	111	111	111	111	111	111	111
820617.	111	111	111	111	111	111	111	111	101	111	111	111	111	111	101	111	111	111	111	111	111	111	111	111
820618.	111	111	111	111	111	111	111	111	111	111	111	111	111	111	111	111	111	111	100	000	000	000	000	000
820619.	000	000	000	000	000	000	000	000	111	111	111	111	111	111	111	111	111	111	111	111	111	111	111	111
820620.	111	111	111	111	111	111	111	111	111	111	111	111	111	111	111	111	000	000	000	000	000	000	000	000

FIG. 8. Sample printout of "Available Data Listing" for M Data (i.e., 20 min summary listing of the type shown in Fig. 9).

sequence (10–300 m) from bottom to top. The number to the left represents the observed mean for the period while the separation between the reference lines represents a velocity scale of 2 m s^{-1}. Note the presence of gravity waves above 100 m and the initiation of convection from surface heating after 0700 MST. Variations of this program for plotting data recorded in the RAW mode and those on special channels are also available.

4) AUTOCORRELATIONS AND LAGGED CROSS-CORRELATIONS

This program computes autocorrelations of variables at individual levels and lagged cross-correlations between levels. Fig. 11 shows one such example for w. This period corresponds to the time series in Fig. 10; wave motions above 100 m produce the oscillations apparent in both correlation plots.

5) SPECTRUM ANALYSIS

Three spectrum analysis programs are available. The first combines the S Data on file with the spectrum computed from the A Data, as described earlier in the paper. The crossover is set at 0.025 Hz. The program operates on pairs of variables, e.g., vertical velocity and temperature, as shown in Fig. 12. All eight levels are plotted in turn.

The second program permits pairing of any standard tower variable with data on a special channel. The third program accepts data directly from tapes

BOULDER ATMOSPHERIC OBSERVATORY DATA SUMMARY

AVERAGING PERIOD= 20.00 MIN 13 OCT 81 1420 MST

	SONIC					PROPVANE				
Z[M]	VWES	VSOU	W	VH	AZ	SPD	DIR	T	TD	L
10	-2.41	-0.04	-0.03	2.42	89.	2.37	76.	5.91	3.99	-42.33
22	-2.91	-0.06	-0.33	2.91	89.	2.61	80.	5.64	3.72	-52.16
50	-3.11	-0.33	0.21	3.13	84.	2.81	82.	5.22	3.98	-53.64
100	-3.20	-0.23	0.45	3.21	86.	2.91	79.	5.07	4.51	-30.61
150	-3.06	-0.21	0.27	3.07	86.	2.97	78.	4.13	4.22	*******
200	-3.21	-0.38	0.25	3.24	83.	3.13	77.	3.66	3.88	*******
250	-3.21	-0.24	0.03	3.22	86.	3.22	82.	3.39	3.78	*******
300	-3.27	-0.49	-0.18	3.30	81.	3.27	80.	3.10	3.17	*******

Z[M]	UU	VV	WW	TT	UV	VW	UT	VT	UW	WT
10	0.4815	0.4314	0.1027	0.0644	-0.0024	-0.0364	-0.0806	0.0027	-0.0833	0.0462
22	0.5538	0.4069	0.1699	0.0412	-0.0082	-0.0271	-0.0628	-0.0065	-0.1068	0.0544
50	0.3823	0.4277	0.2772	0.0159	0.0150	0.0025	-0.0201	-0.0043	-0.0816	0.0353
100	0.3424	0.3281	0.3938	0.0086	0.0293	-0.0822	-0.0211	-0.0036	-0.0507	0.0302
150	0.2828	0.1896	0.3683	0.0055	-0.0321	-0.0447	-0.0059	-0.0016	0.0187	0.0241
200	0.2619	0.2516	0.4432	0.0030	-0.0303	-0.0743	0.0007	0.0028	0.0776	0.0178
250	0.3662	0.2598	0.5077	0.0016	-0.0734	-0.1648	0.0035	-0.0036	0.1172	0.0182
300	0.4162	0.4147	0.5216	0.0018	-0.0641	-0.1784	0.0115	-0.0082	0.2503	0.0213

OPTICAL TRIANGLE				PRESSURE STAND. DEV. [MICROBARS]				
V [M/SEC]	AZ[DEG]	CONV[1/SEC]	LOG10 CN-SQR	STN 1	STN 2	STN 3	STN 4	STN 5
1.79	75.	0.00183	-14.84266	1.686	5.255	1.590	2.976	4.463

PRESSURE[MB] 837.10

SOLAR RAD[LY/MIN] 0.12

FIG. 9. Twenty-minute summary listing for period starting 1420 MST on 13 October 1981. See text for explanation of parameters listed.

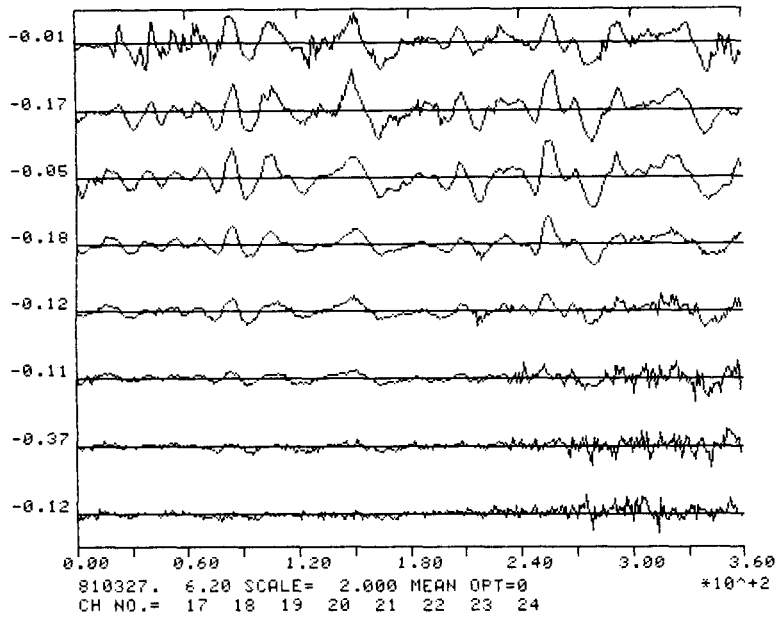

FIG. 10. Plots of the vertical velocity component at the eight fixed levels on the tower for 1 h starting 0620 MST on 27 March 1981. The plots comprise 360 data points per level, retrieved from the archived A Data. The period shows onset of convective activity at the three lowest levels.

recorded at the BAO site in the RAW mode. Spectra and cospectra of all wind components and temperature are computed over periods ranging from 2 min to 1 h 40 min. (Note: quadrature spectra are calculated in all cases, but not plotted.)

6) PROBABILITY DISTRIBUTIONS

The probability distribution of any desired variable is plotted as a function of specified bin range for all eight levels on the tower. Printed listings of the distributions along with standard deviations, skewness and kurtosis for the period are provided with the plot.

7) WIND CLIMATOLOGY

Wind roses, frequency distributions of windspeed and wind direction, covering time intervals from 1 day to 1 year, are constructed for all eight levels. The output includes both plots and listings.

8) SCATTER DIAGRAM

A highly useful presentation for comparing performance of like sensors, this program is used extensively in intercomparison experiments. The variables plotted on the abscissa and the ordinate can be selected from any channel in the A Data file.

9) BEAM-STEERING PROGRAM

A special program to estimate the speed and direction of gravity waves is available. It uses as input microbarograph measurements and plots contours of cross-correlation in polar coordinates where the radial dimension is the reciprocal of velocity and the azimuth angle is defined in the conventional manner, increasing clockwise (see Fig. 13). The origin represents infinite phase velocity, while the coordinates of the point of maximum correlation represent the phase velocity and direction of the wave. Cross-correlation contours are obtained by phase shifting pairs of pressure signals from the microbarograph stations. At least three spatially separated measurements are needed to calculate the wave parameters. The program also allows variable band-pass filtering to isolate individual spectral bands when more than one frequency is present.

10) OTHER

The BAO software library also includes programs for transcribing data from one form to another: 1) converting data recorded on tape (RAW or REG modes) to the standard format for storage on disk files, and 2) converting data in archived tapes to standard ASCII 80 characters per second, card image format, for use on other computer systems. The latter form is used primarily to extract selected channels of data for outside users of BAO data.

5. BAO research program

In four years of operation the BAO staff has coordinated and executed some major field experiments

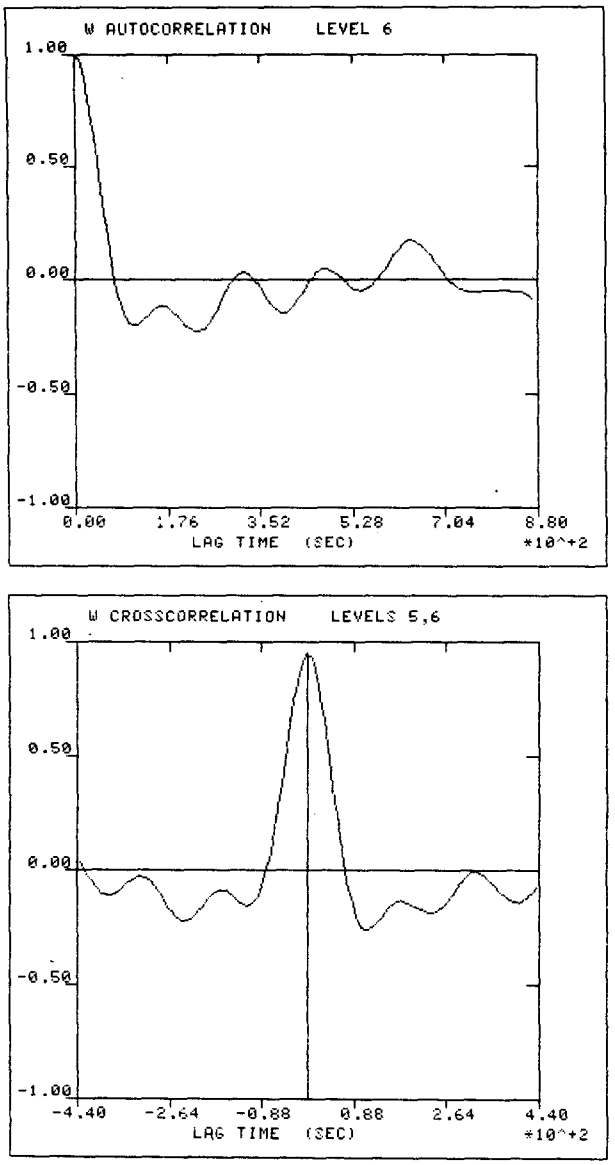

FIG. 11. Plots of the autocorrelation function for the vertical velocity component at 200 m (above) and the lagged cross correlation between the same component measured at 150 and 200 m (below).

and several smaller ones. The first major experiment was conducted jointly by scientists in WPL, NCAR and the University of Washington during April of 1978. Known as the BAO Site Evaluation Experiment, its aim was to determine how the unevenness of the terrain influenced the temporal and spatial structure of the boundary layer over the site. In addition to observations from the newly instrumented tower, the experiment utilized aircraft (NCAR Queen Air) measurements of wind and temperature turbulence along two orthogonal flight legs centered around the tower and data from a network of 28 surface sta-

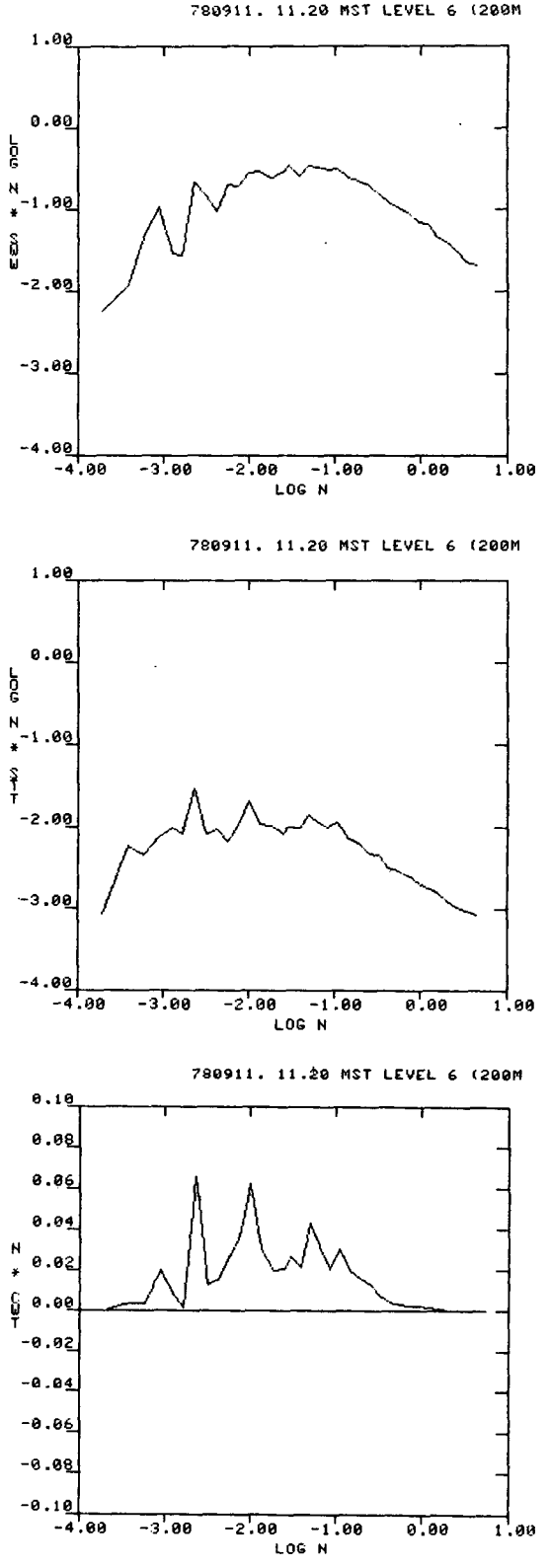

FIG. 12. Spectra of vertical velocity component and temperature (top two) and cospectrum of vertical temperature flux (bottom) at 200 m for a 1 h 40 min period starting 1129 MST on 11 September 1979. These spectra are typical for the convective boundary layer.

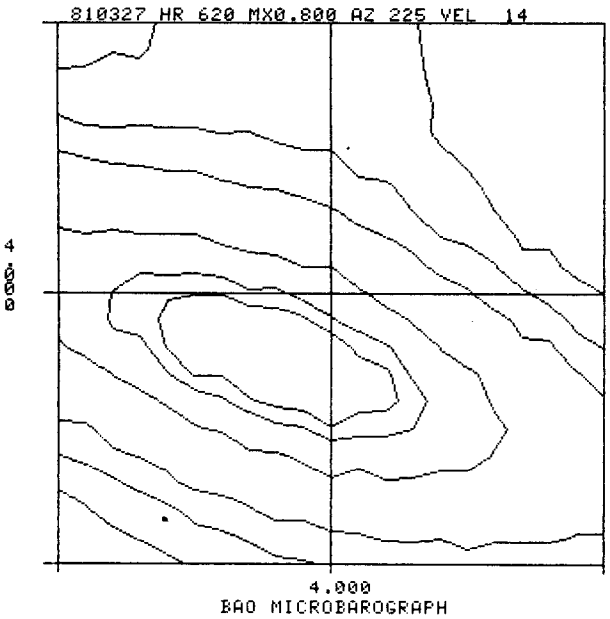

FIG. 13. Plotted output of the microbarograph beam-steering program showing contours of cross correlations between pairs of stations. In the presence of a gravity wave, the plot indicates a maximum value at coordinates corresponding to the phase velocity and direction of the wave (14 m s^{-1} from 225° azimuth in this case). Distance from the origin represents the reciprocal of the phase velocity, while the clockwise angle from north represents the direction from which the wave approaches the stations.

tions (NCAR's Portable Automated Mesonet) measuring windspeed, wind direction, temperature and pressure. The study by Kaimal *et al.* (1982b) of the convective boundary layer behavior indicates a structure very similar to that observed over flat terrain. Concurrent measurements of convective plumes from the tower sensors and a horizontal array of 16 fast-response temperature sensors resulted in a definitive study of plume structure and transport by Wilczak and Tillman (1980). Using 20 min summary data collected round the clock during the same experiment period, Hahn (1981) examined wind flow patterns at the BAO and found diurnal wind oscillations favored on days when the synoptic geostrophic wind is southerly.

A second field experiment was conducted the same year in September to study the evolution and decay of the convective boundary layer. This project, named PHOENIX for the mythical bird that rose from its ashes each morning, brought together scientists from the different NOAA laboratories in Boulder, the NOAA Atmospheric Turbulence and Diffusion Laboratory in Oak Ridge, Tenn., the Jet Propulsion Laboratory and NCAR. All available remote sensors in the Boulder area, the NCAR aircraft, and the NCAR PAM network participated, providing their different inputs to the data base. Details of the experiment can be found in a special report, edited by Hooke (1979).

A broad range of studies have emerged from the PHOENIX Experiment. Kaimal *et al.* (1982a) described a comparison of eight different techniques, three *in-situ* and five remote, to measure boundary layer thickness. Wind fields measured by dual-Doppler radars were compared with *in-situ* measurements from aircraft, tower and other surface wind sensors by Kropfli and Hildebrand (1980); Tsay *et al.* (1980) reported comparisons of convergence measurements from the optical triangle with vertical velocity gradients from the tower. Using data from neutral balloon trajectories tracked by double theodolites and the X-band radar, Hanna (1980) developed relationships between Lagrangian and Eulerian time scales valid for horizontal scales of turbulence at all heights in the mixed layer.

An important study of the interaction between internal gravity waves and turbulence, described by Einaudi and Finnigan (1981) and Finnigan and Einaudi (1981), was based on the analysis of a near-monochromatic wave event observed during the early hours of the morning. The monochromatic nature of the pressure signal at the ground made possible an explicit separation of the velocity field into its mean, turbulent and wave components.

The experiment offered Decker *et al.* (1981) the opportunity to study the effect of gravity waves on passive radiometric measurements in the water vapor and oxygen absorption bands. Three passive radiometric devices developed for retrieval of tropospheric temperature and humidity profiles were compared (Decker, 1979), and the increase in accuracy gained through supplementary information on the height of the boundary layer was demonstrated.

Pasqualucci and Abshire (1980) found good agreement between measurements of cloud top and cloud base made with the 8 mm TPQ-11 radar and the lidar. A comparison of radar and lidar reflectivities directly observed and calculations based on drop-size distribution spectra measured by an airborne Knollenberg probe show differences which are discussed by Pasqualucci *et al.* (1980).

The third major experiment took place during August and September of 1979 under WMO auspices. Known as the Boulder Low-Level Intercomparison Experiment (BLIE), its objective was to establish compatibility between the various low-level sounding techniques developed in recent years. The types of instruments compared included acoustic sounders, radiosonde and tethersonde packages of both domestic and foreign construction, a remotely piloted aircraft from France, a tower instrumentation system from Finland, a sonic anemometer-thermometer system from Japan, and a hybrid radio-acoustic sounding system from Switzerland. Eleven WMO member nations participated with equipment and as observers. The experiment and the associated workshop were organized jointly by WPL and NCAR. A report

detailing the workshop proceedings and the test results is available (Kaimal *et al.*, 1980a).[8] For a concise summary of the experiment see Kaimal *et al.* (1981). More details on the radiosonde intercomparisons are given by Baynton *et al.* (1981).

Studies of mean wind characteristics at the BAO were carried out by Panofsky and his coworkers at Pennsylvania State University using data from the two 1978 experiments (Schotz and Panofsky, 1980; Korrell *et al.*, 1982). The studies found surface layer theory to be adequate without modification for west winds but not for winds from the south and southeast. Estimation of windspeeds to a height of 150 m from windspeed and stability information at 10 m was found possible with similarity theory for $z/L < 0.1$. Meanwhile, data from two high-wind episodes observed along the Front Range and at the BAO tower were analyzed by the BAO staff to develop statistics for testing the validity of two gust models developed by the Battelle Pacific Northwest Laboratory for design of large wind turbine generators. This study is described by Kaimal *et al.* (1980b).

Much work has been conducted at the BAO site by visiting scientists and personnel from other institutions. Sievering (1981) and Ganor and VanValin (1982) report studies of the vertical profiles of particulates and gases observed from the BAO tower. The BAO resources have been used to check calibrations of the NCAR research aircraft, Boeing Aircraft Company's test aircraft, Stanford Research Institute's DIAL lidar system, the U.S. Department of Transportation's airborne and ground-based lidar wind sensors, to name a few. Preliminary tests have begun in collaboration with the Federal Aviation Administration to conduct wake vortex studies from aircraft, using a combination of tower sensors, FM-CW radar and microbarographs, with smoke releases, for flow visualization of the vortices.

The following experiments are in progress or scheduled at the BAO:

1) STABLEX, a study aimed at examining relationships between fluxes and gradients (over a 10 m vertical separation) measured from the carriage positioned at various heights within the nocturnal stable layer.

2) BUCOE (Boulder Upslope Cloud Observation Experiment) conducted jointly by NOAA laboratories and NCAR during the spring of 1982 to observe the role of ice crystals and cloud microphysics in the evolution of upslope precipitation and to calibrate various remote sensing systems against reliable *in-situ* devices on the tower and on aircraft.

3) Turbulence Sensor Intercomparison for EPA to assess performance of tower-based *in-situ* and acoustic Doppler systems. A major focus will be the evaluation of data processing techniques used for calculating "equivalent standard deviations" from wind data. The experiment was conducted in September 1982.

4) Convective Diffusion Field Experiment under EPA sponsorship and planning, to study the transport of oil fog and aluminized chaff plumes released simultaneously from the ground and the top of the BAO tower. The plumes are tracked by the dual-channel lidar and the X-band radar, respectively. A preliminary experiment to test the feasibility of the remote sensing techniques was conducted in September 1982; the full experiment is planned also for September 1983.

6. Concluding remarks

Since its inception in April 1978 the BAO has served the needs of a broad range of users, from boundary layer scientists and designers of new remote sensors to operators of instrumented aircraft and standard surface air monitoring systems. Data sampling and processing procedures are designed for continuous data acquisition and real-time displays of summary information. BAO's multi-user data processing and archiving system permits easy access to current as well as past data. Programs used most frequently for analyzing and plotting boundary layer data now reside as standard library routines in computer memory.

The present blend of major field experiments, small-scale experiments, and data analysis will continue at the BAO. The facility was designed with external users in mind; interested researchers are invited to participate in any aspect of ongoing programs or to pursue, working with the BAO staff, ideas for new experiments. The BAO staff looks forward to continued cooperation with universities, government agencies and other institutions.

Data acquisition at the BAO proceeds on a continuous basis even during periods between experiments. The data recovery rate for archiving is approximately 85%. Although staff limitations restrict our ability to respond to data requests, access to the BAO computer terminals and to our archived data tapes can be arranged for scientists and students planning to visit the area.

APPENDIX A

Transducer Shadow Correction for an Orthogonal Horizontal Sonic Anemometer Array

In a fixed sonic anemometer array, like that used at the BAO, correction is made for underestimation of the measured velocity component u_m, due to partial shadowing of the acoustic path by the transducers. An approximate form for the velocity underestimation, as a function of θ (angle between the wind di-

[8] Also available as WMO Instruments and Observing Methods, Report No. 3, 1980.

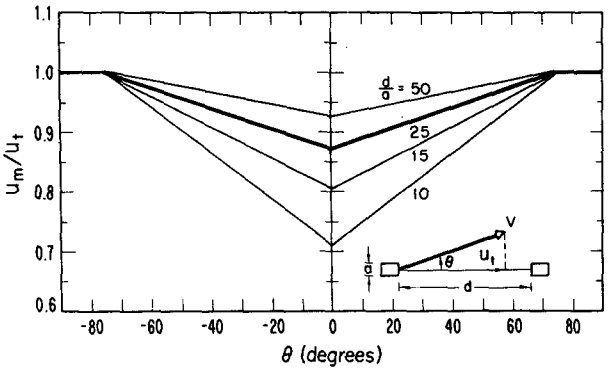

FIG. 14. Attenuation in sonic anemometer wind velocity component from flow distortions along the acoustic path introduced by the transducers. The heavy line, corresponding to d/a = 25, represents the response curve for the BAO anemometers.

rection and the acoustic path), has been obtained from wind tunnel and atmospheric tests (see Fig. 14). The measured velocity component u_m approaches the true velocity component u_t in the range $75° > \theta > 90°$ but drops off linearly with θ for angles $< 75°$. For an aspect ratio (path length/transducer diameter) of 25, appropriate to the array,

$$u_m = \begin{cases} u_t(0.87 + 0.13\theta/75), & 0 \leq \theta \leq 75 \\ u_t, & 75 \leq \theta \leq 90 \end{cases} \quad \text{(A1)}$$

While an arc tangent routine can be used for a first-order approximation of θ (from wind components u_m and v_m measured along the two axes), it is more efficient to compute u_t and v_t using analytical expressions given below that very nearly approximate (A1). Defining u_t as the component more closely aligned with the wind and v_t as the component normal to it, we have

$$u_t = Cu_m, \quad \text{(A2a)}$$

$$v_t = Dv_m, \quad \text{(A2b)}$$

where

$$C = 0.926 + 0.31/(R + 1.38), \quad \text{(A3a)}$$

$$D = \begin{cases} 2.112 - C, & D > 1 \\ 1.0, & D \leq 1 \end{cases} \quad \text{(A3b)}$$

$$R = |v_m|/|u_m|. \quad \text{(A3c)}$$

No such correction is applied to the vertical velocity component.

APPENDIX B

Block Averaging of FFT Spectral Estimates in the BAO Spectrum Analysis Routine

The smoothness of the BAO spectral plots result from block-averaging spectral estimates to provide a roughly logarithmic spacing between data points. The grouping of the FFT spectral estimates for the on-site spectral calculations with 10 Hz sampled data and the low-frequency spectral calculations with the 10 s block-averaged time series in the A Data file are given in Tables 3 and 4. The center frequency n_c is computed as follows:

$$n_c = \frac{k_c \times (\text{sampling rate})}{(\text{total number of samples})},$$

where k_c is the estimate number assigned to the block. Thus

$$n_c = k_c \times 10/1024,$$

for the high-frequency spectral calculations ($0.025 < n < 0.5$ Hz) and

$$n_c = k_c \times 0.1/516,$$

for the low-frequency spectral calculations ($0.0002 < n < 0.025$ Hz).

The blocking-averaging schemes used for smoothing the two spectra are given in Tables 3 and 4.

Note that the 0th estimate is omitted in both tables. Transition from the high- to the low-frequency set of estimates occurs at n_c = 0.025 Hz in the plotting routine. The high-frequency estimates plotted are the averages of estimates listed in the S data file covering the period analyzed (3–5 20 min output periods). The program accomodates time series of variable length

TABLE 3. Spectral smoothing for the 1024-point FFT calculations.

No.	Contents in each block (in estimate number, k)	Number of estimates per block	Center of block k_c	Center frequency n_c (Hz)
1	1	1	1	0.0098*
2	2	1	2	0.0195*
3	3	1	3	0.0293
4	4	1	4	0.0391
5	5	1	5	0.0483
6	6–7	2	6.5	0.0634
7	8–9	2	8.5	0.0831
8	10–12	3	11	0.1074
9	13–16	4	14.5	0.1416
10	17–22	6	19.5	0.1904
11	23–28	6	25.5	0.2490
12	29–37	9	33	0.3223
13	38–48	11	43	0.4199
14	49–63	15	56	0.5469
15	64–82	19	73	0.7129
16	83–107	25	95	0.9277
17	108–139	32	123.5	1.2061
18	140–180	41	160	1.5625
19	181–234	54	207.5	2.0264
20	235–303	69	269	2.6270
21	304–394	91	349	3.4082
22	395–511	117	453	4.4238

* Deleted in plotting routines.

TABLE 4. Spectral smoothing for the 516-point FFT calculations.

No.	Contents in each block (in estimate number, k)	Number of estimates per block	Center of block k_c	Center frequency n_c (Hz)
1	1	1	1	0.000195
2	2	1	2	0.000391
3	3	1	3	0.000586
4	4–5	2	4.5	0.000879
5	6–7	2	6.5	0.001269
6	8–9	2	8.5	0.001660
7	10–13	4	11.5	0.002246
8	14–18	5	16	0.003125
9	19–24	6	21.5	0.004199
10	25–32	8	28.5	0.005566
11	33–43	11	38	0.007422
12	44–58	15	51	0.009961
13	59–79	21	69	0.013477
14	80–106	27	93	0.018164
15	107–142	36	124.5	0.024316
16	143–190	48	166.5	0.032520*
17	191–255	65	223	0.043555*

* Deleted in plotting routines.

from the A data file (3–5 output periods) to compute the low-frequency estimates.

REFERENCES

Baynton, H. W., J. C. Kaimal, J. E. Gaynor, D. B. Call, I. Ikonen and E. Schöllmann, 1981: Field experience with a new method of comparing radiosonde systems. Papers presented at the Second WMO Tech. Conf. Instruments and Methods of Observation (TECIMO II), WMO Instruments and Observing Methods Rep. No. 9, 123–130.

Bedard, A. J. Jr., 1982: Sources and detection of atmospheric wind shear. *AIAA J.*, **20,** 940–945.

——, and C. Ramzy, 1979: Microbarograph observations during PHOENIX. *Project PHOENIX—The September 1978 Field Operation,* W. H. Hooke, Ed., BAO Rep. No. 1, 150–156.*

Decker, M. T., 1979: Microwave radiometric studies in PHOENIX. *Project PHOENIX, The September 1978 Field Operation,* W. H. Hooke, Ed. BAO Rep. No. 1, 69–79.*

——, F. Einaudi and J. J. Finnigan, 1981: The influence of gravity waves on radiometric measurements: A case study, *J. Appl. Meteor.*, **20,** 1231–1238.

Einaudi, F., and J. J. Finnigan, 1981: The interaction between an internal gravity wave and the planetary boundary layer. Part I: The linear analysis, *Quart. J. Roy. Meteor. Soc.*, **107,** 793–806.

Finnigan, J. J., and F. Einaudi, 1981: The interaction between an internal gravity wave and the planetary boundary layer. Part II: Effect of the wave on the turbulence structure. *Quart. J. Roy. Meteor. Soc.*, **107,** 807–832.

Ganor, E., and C. C. VanValin, 1982: Vertical profiles of gases and particles in the nonurban atmosphere. *Preprints Second Symp. Composition of the Non-Urban Troposphere,* Williamsburg, Amer. Meteor. Soc., 214–217.

Hahn, C. J., 1981: A study of the diurnal behavior of boundary layer winds at the Boulder Atmospheric Observatory. *Bound.-Layer Meteor.*, **21,** 231–245.

Hall, F. F., Jr., 1977: The Boulder Atmospheric Observatory. *Opt. News,* **3,** No. 2, 14–18.

Hanna, S. R., 1980: Lagrangian and Eulerian time-scale relations in the dyatime boundary layer. *J. Appl. Meteor.*, **20,** 242–249.

Haugen, D. A., 1978: Effects of sampling rates and averaging period on meteorological measurements. *Preprints Fourth Symp. Meteorological Observations and Instrumentation,* Denver, Amer. Meteor. Soc., 35–40.

Hooke, W. H., Ed., 1979: *Project PHOENIX—The September 1978 Field Operation,* BAO Rep. No. 1, 281 pp.*

Kaimal, J. C., J. C. Wyngaard, Y. Izumi and O. R. Coté, 1972: Spectral characteristics of surface layer turbulence. *Quart. J. Roy. Meteor. Soc.*, **98,** 563–589.

——, J. T. Newman, A. Bisberg and K. Cole, 1974: An improved three-component sonic anemometer for investigation of atmospheric turbulence. *Flow—Its Measurement and Control in Science and Industry,* Vol. 1, Instrum. Soc. Amer., 349–359.

——, H. W. Baynton and J. E. Gaynor, Eds., 1980a: The Boulder low-level intercomparison experiment. BAO Rep. No. 2, 189 pp.*

——, J. E. Gaynor and D. E. Wolfe, 1980b: Turbulence statistics for design of wind turbine generators. BAO Rep. No. 3, 102 pp.*

——, ——, H. W. Baynton and F. G. Finger, 1981: The Boulder low-level intercomparison experiment. *Papers presented at the Second WMO Tech. Conf. Instruments and Methods of Observation (TECIMO II),* WMO Instruments and Observing Methods Rep. No. 9, 167–174.

——, N. L. Abshire, R. B. Chadwick, M. T. Decker, W. H. Hooke, R. A. Kropfli, W. D. Neff, F. Pasqualucci and P. H. Hildebrand, 1982a: Estimating the depth of the daytime convective boundary layer. *J. Appl. Meteor.*, **21,** 1123–1129.

——, R. A. Eversole, D. H. Lenschow, B. B. Stankov, P. H. Kahn and J. A. Businger, 1982b: Spectral characteristics of the convective boundary layer over uneven terrain. *J. Atmos. Sci.*, **39,** 1098–1114.

Korrell, A., H. A. Panofsky and R. J. Rossi, 1982: Wind profiles at the Boulder tower. *Bound.-Layer Meteor.*, **22,** 295–312.

Kropfli, R. A., and P. H. Hildebrand, 1980: Three-dimensional wind measurements in the optically clear planetary boundary layer with dual-Doppler radar. *Radio Sci.*, **15,** 283–296.

Mitsuta, Y., 1974: Sonic anemometer thermometer for atmospheric turbulence measurements. *Flow—Its Measurement and Control in Science and Industry,* Vol. 1, Instrum. Soc. Amer., 341–347.

Moninger, W. R., and R. A. Kropfli, 1982: Radar observations of a plume from an elevated continuous point source. *J. Appl. Meteor.*, **21,** 1685–1697.

Pasqualucci, F., N. L. Abshire, R. B. Chadwick and R. A. Kropfli, 1980: Cloud observations during the PHOENIX experiment. *Preprints Nineteenth Conf. Radar Meteorology,* Miami Beach, Amer. Meteor. Soc., 716–717.

——, and ——, 1980: A comparison of cloud top and cloud base measurements by lidar and 8.6-mm radar. *Preprints Nineteenth Conf. Radar Meteorology,* Miami Beach, Amer. Meteor. Soc., 718–721.

Schotz, S., and H. A. Panofsky, 1980: Wind characteristics at the Boulder Atmospheric Observatory. *Bound.-Layer Meteor.*, **19,** 155–164.

Sievering, H., 1981: Profile measurements of particle dry deposition velocity in an air/land interface. *Atmos. Environ.*, **15,** 301–306.

Tsay, Mu-King, Ting-I Wang, R. S. Lawrence, G. R. Ochs and R. B. Fritz, 1980: Wind velocity and convergence measurements at the Boulder Atmospheric Observatory using path-averaged optical wind sensors. *J. Appl. Meteor.*, **7,** 826–833.

Wilczak, J. M., and J. E. Tillman, 1980: The three-dimensional structure of convection in the atmospheric surface layer. *J. Atmos. Sci.*, **37,** 2424–2443.

* Available from NOAA/ERL/Wave Propagation Laboratory, Boulder, CO.